On-site Measurement of Complex Waveforms on Transmission Network Components

Peter Wouters, Armand van Deursen,
Jeroen van Oorschot and Marcel Hoogerman
Eindhoven University of Technology
Eindhoven, the Netherlands

Bernd van Maanen
DNV Energy
Arnhem, the Netherlands

Abstract

Superimposed voltage waveforms may result in electrical stresses in dielectric materials not anticipated for. Non-intrusive methodologies to observe these events, both capacitively and inductively, are discussed. This paper presents two examples where complex waveforms arise from energizing and de-energizing inductive loads. Case I: A compensation coil connected through overhead lines showed high overvoltage levels when being energized by means of a SF_6 switchgear. Case II: A compensation coil connected via a power cable with a vacuum switchgear experienced high overvoltage levels from recurrent restrikes during its de-energization.

1. Introduction

Combined voltage waveforms are becoming frequent events due to increased switching related to the operation of distributed power generation. Their peak voltage level and frequency content may harm insulation materials in network components.

Energization and de-energization events in transmission grids are examples of superimposed voltage waveforms involving a fast transient voltage on top of the power frequency voltage. These waveforms may contain frequency components reaching up to the megahertz range. This paper investigates their presence by field measurements and their detection by means of capacitive or inductive sensors. Wideband recording of these events is challenging as the measurement must be performed safely, should be non-invasive and need to have good characteristics concerning electromagnetic compatibility (EMC).

In Section 2, aspects related to on-site measurement on components without integrated voltage sensing facilities are discussed. Two situations where potentially high overvoltages occur are described in Sections 3 and 4. These situations relate to switching of a compensation coil in high voltage transmission grids. These coils are connected to or disconnected from the tertiary windings of a transformer to reduce transmission losses, depending on the momentary power consumption (e.g., on a daily base for day/night cycles) or depending on the power generation (irregularly in case of wind farms). The investigated cases are:

- Case I: 380/220/50 kV transformer with the coil connected via overhead lines and employing SF_6 switchgears
- Case II: 380/220/33 kV transformer with the coil connected via underground cables using vacuum switchgears

2. Measurement options

Transient overvoltages in power equipment without pre-installed voltage measurement facilities can be obtained from the parasitic capacitive coupling to the phase conductors. The charge induced in a sensor, e.g. a metal plate positioned at a safe distance, is a measure for the voltage level. However, the magnitude of the coupling strength is, at most, roughly known and a calibration procedure is needed. As the coupling may be weak, the signal levels can be low, and a good EMC design is key for reliable results.

A parasitic capacitance can be employed as the high-voltage branch as part of a capacitive divider (Section 2.1). Alternatively, the low-voltage branch of such divider can be omitted, and the input of the detection system makes up this impedance (Section 2.2). The signal then represents the time derivative of the signal, and the waveform needs to be restored by integration.

For closed systems, there is no direct access to the electric fields emerging from the system. This is the case when the connection between the compensation coil and the switchgear is accomplished by a shielded power cable. The voltage waveform can be retrieved from the charging current of such cable by means of a high frequency current transformer (HFCT) around the cable earth connection (Section 2.3). Also here, the signal will represent the time-derivative voltage and integration is needed. Such methods are referred to as differentiating-integrating (D-I) techniques [1]. They will be discussed with respect to their sensitivity, selectivity and EMC.

2.1. Capacitive divider

The capacitive divider configuration with connection to the recording device is depicted in Fig. 1a. Capacitor C_1 represents the parasitic sensor capacitance, and its value can be in the order of 1 pF. The value of C_2 in the low-voltage branch determines the division ratio. The input impedance of the recording equipment should be sufficiently high in order not to affect the division ratio. Consequently, the measurement cable cannot be terminated by its characteristic impedance. With longer cable lengths (tens of metres), such configuration is not suitable for measuring fast transient signals, due to travelling waves up and down the measurement cable.

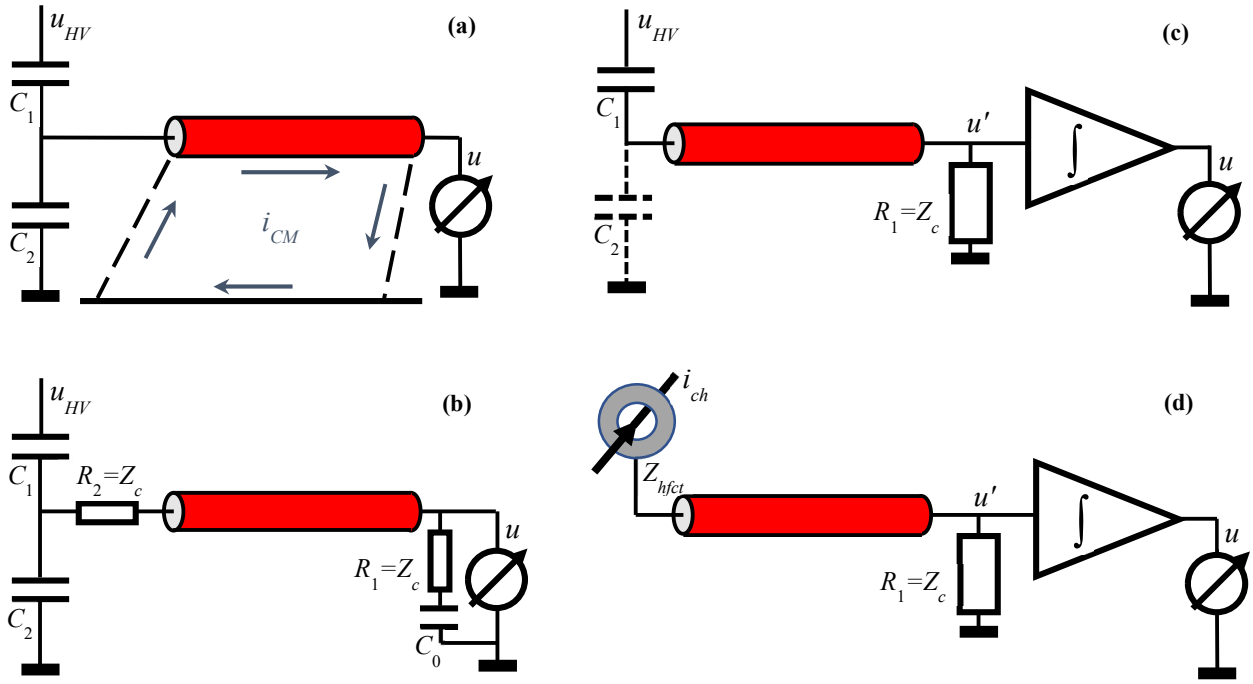

Fig. 1 – Measurement configurations with (a) capacitive divider and influence of a common mode current i_{CM}, (b) divider with improved high frequency response, (c) capacitive D-I measurement circuit, (d) inductive D-I measurement circuit

Improvement of the high-frequency response is obtained by the configuration of Fig. 1b [2]. The resistances are equal to the characteristic cable impedance Z_c. With $C_0+C_c = C_1+C_2$ (C_0 an additional capacitor at the receiving cable end and C_c the cable capacitance), the division ratio is equal for low and high frequency. Distortion may still occur in some intermediate frequency range.

Switching transients cause high system current magnitudes, which can induce common mode (CM) currents i_{CM}. Measurement cabling is susceptible to such induced currents. Through the transfer impedance Z_t of the measurement connection, an unintended voltage equal to i_{CM} times Z_t will arise, which adds to the signal from the sensor [3]. This voltage divides over the impedances at the ends of the measurement cable, with the main part dropping over the highest value. In the configuration of Fig. 1a this is at the receiving end, where the measurement takes place. For the high frequency range in case of Fig. 1b, the termination impedance is mainly determined by the resistances R_1 and R_2, which are taken equal to Z_c. Then, the disturbing voltage divides equally over both ends.

2.2. D-I capacitive measurement

For the D-I approach in Fig. 1c, the measurement cable is an integral part of the measurement circuit. It is characteristically terminated at the receiving end and the response will be the time derivative up to the cut-off frequency given by $1/2\pi R_1(C_1+C_2)$. The capacitor C_2 can either be the parasitic capacitance from the sensor to ground or part of the circuit design aiming for a defined high-frequency cut-off frequency [4]. An integrator restores the waveform. The hybrid passive/active design from [1] is used, having an integrating response between about 10 Hz and 20 MHz.

For frequencies below the high frequency cut-off, the impedance at the sensor side of the measurement cable (mainly determined by C_2) is higher than the impedance at the recording side (R_1 = 50 Ω). Disturbing signals from CM currents will therefore arise at the sensor end rather than at the measurement end. In addition, high frequency interfering signals entering the measurement cable will be weakened by the integration step. The use of parasitic capacitances as sensors and the good EMC properties make that the D-I approach is suitable for non-invasive measurement of transient voltages involving large and steep wave fronts. A drawback is that a sensor not only receives a signal from the intended phase conductor, but also from the other phases. Signal decoupling methods together with their accuracies are described in [4].

2.3. D-I inductive measurement

Capacitive coupling cannot be used for a compensation coil connected via a power cable. In case of a single-sided ground connection, it carries the cable charging current i_{ch}, which represents the time-derivative of the voltage. For this approach, the power cable capacitance is employed as sensor and the current is measured by means of a HFCT, as shown in Fig. 1d. The HFCT type is selected for sufficient sensitivity, large bandwidth, its capability of handling high peak currents (Z_{hfct} = 0.1 Ω, 50 MHz, 5 kA, [5]), and for good shielding.

A disadvantage is that the power cable length becomes the limiting factor for the bandwidth due to signal transit times. The system studied in Section 4 has a cable length in the range of 30 to 40 m, meaning that transmission line effects can only be neglected up to a frequency of several

megahertz. Also, the impedance at the output of the employed HFCT is much lower than the termination resistance R_1 (50 Ω), meaning that interference related to a CM current can arise at the receiving end of the measurement cable. Interference from high frequency signals, picked up by the measurement cable, is still reduced by the integration step. The HFCTs are selective since they respond only to the charging current of the phase conductor where they are installed.

Fig. 2 – Compensation coil (left) and capacitive sensor positioning beneath the overhead lines connecting the compensation coil to the switchgears (right)

3. Case I: capacitive measurement

Fig. 2 shows a 50 kV compensation coil (left) and the connecting lines to the switchgear with the capacitive sensors (right). The sensors are positioned underneath the phase conductors. The sensors (30×30 cm^2) are designed to have about 1 pF coupling capacitance. The sensors are connected via 25 m long measurement cables to the integrators. The recorded signal according to Fig. 1c is (for signal frequencies below the cut-off frequency):

$$\left.\begin{aligned} u'(t) &= R_1 C_1 \frac{\mathrm{d}u_{HV}(t)}{\mathrm{d}t} \\ u(t) &= \frac{1}{\tau_{int}} \int u'(t)\mathrm{d}t \end{aligned}\right\} \Rightarrow u(t) = \frac{R_1 C_1}{\tau_{int}} u_{HV}(t) \qquad (1)$$

With the integration time constant $\tau_{int} = 20$ µs for the employed integrators [1], the power frequency amplitude becomes in the order of 100 mV.

3.1. Signal manipulation

The sensor output for signals with low frequencies become small and integrator instability arises below the power frequency. Fig. 3a shows the recorded waveforms. Besides the offset, also a low frequency variation (several Hertz) can be observed. A digital high-pass filter with cut-off frequency at 25 Hz removes these integrator deviations. Coupling from other circuits result in a small 50 Hz signal visible prior to energization, which can be removed by means of a zero measurement. Fig. 3b shows

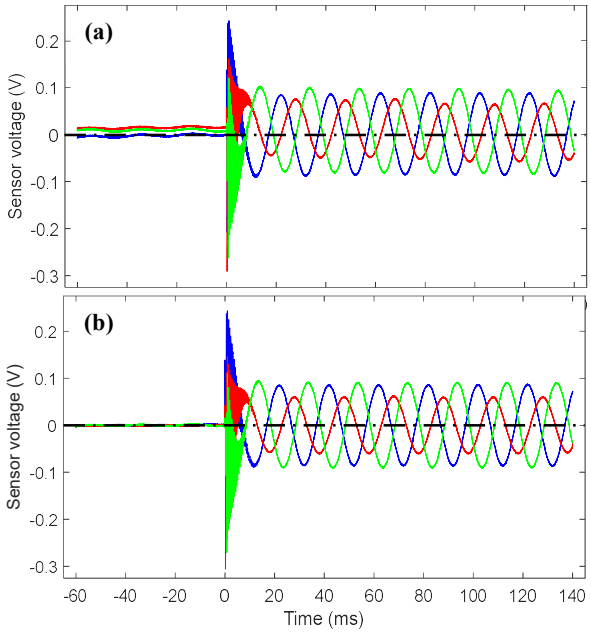

Fig. 3 – Measured energization waveforms (a) before and (b) after filtering the integrator instability and removing the contribution from nearby circuits

the filtered waveforms. The sample rate is 50 Msample/s and the detection bandwidth is about 20 MHz.

The coupling of the sensors to the phase conductors can be formulated in terms of a 3 by 3 matrix [4]. The nine elements are extracted from the following considerations. The power frequency amplitudes are equal (1 p.u.) and the differences between phases are 120º. This provides five conditions, and more information is needed to establish the full coupling matrix. The waveforms during 1 ms around the energization moment in Fig. 4a show that the energization of the phases occurs at distinct times. The relative response of a sensor responding to the energization of a neighbouring phase, compared to the response of the sensor near that phase, is a measure for their relative coupling strength. With this information

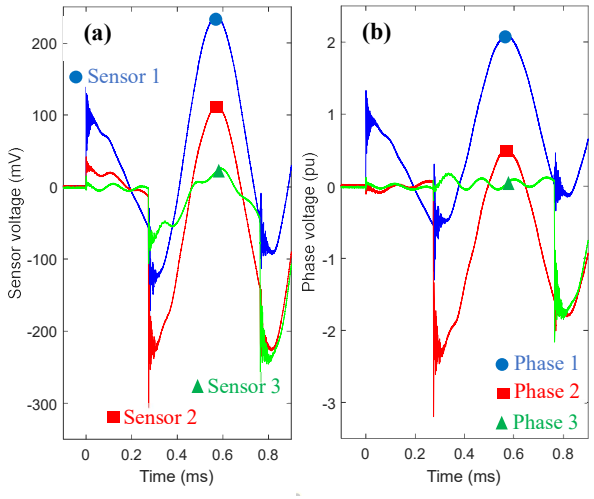

Fig. 4 – Elimination of cross-coupling: (a) waveforms from sensors and (b) reconstructed phase voltages around the switching moment after decoupling

applied to the contact instances of the three phases, the coupling matrix can be established [4]. The decoupled phase voltages upon energization are shown in Fig. 4b.

3.2. Switching overvoltages

The voltage waveforms, during the first power cycle when energizing, are shown in Fig. 5a. The waveform consists of a 2.3 kHz oscillation superimposed on the power frequency signal, which is indicated with the dashed curves. Phase 2 shows an initial overvoltage exceeding 3 p.u. just after energization.

The waveforms for a de-energization event of the compensation coil are shown in Fig. 5b. First, phase 3 shows an overvoltage related to the interruption followed by a restrike near its voltage maximum and a 2.3 kHz oscillation. Later, successful interruption occurs when phase 2 reaches its peak, resulting in a 1.9 kHz oscillation in the still connected phases on top of the power frequency signal. Finally, also these phases interrupt and their voltages quench with an 8 kHz oscillation.

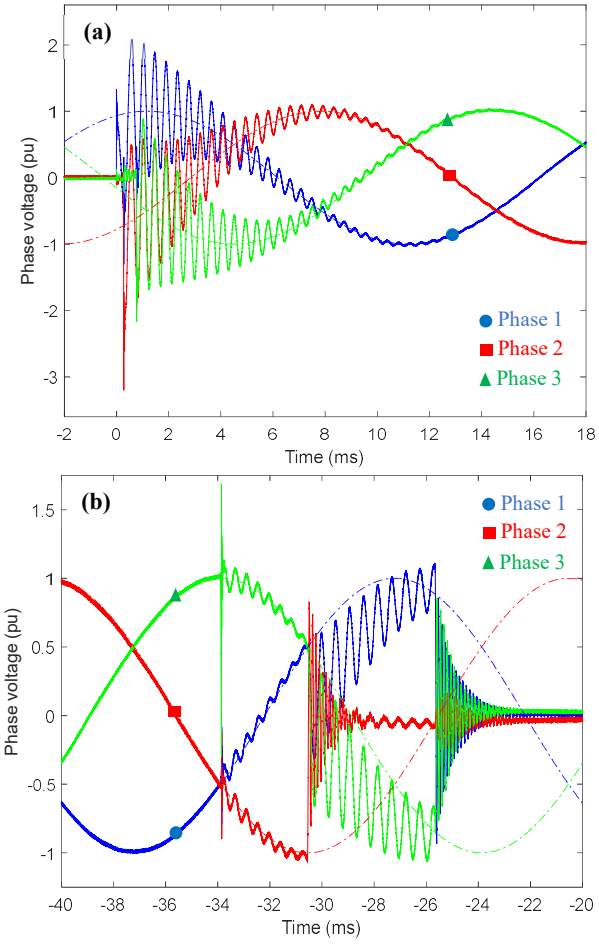

Fig. 5 – Waveform around the switching moment during (a) energization and (b) de-energization

Three energizing and de-energizing events were recorded on two similar compensation coils. The peak voltages are summarized in Table 1. A single restrike occurred in five out of six de-energization recordings. However, the peak values are moderate as compared to the maximum overvoltage registered during energization.

Table 1 – Peak voltages registered in recordings of switching events for two compensation coils (A and B)

Coil	Peak voltage energization (p.u.)	Peak voltage de-energization (p.u.)
A	-3.2 (phase 2); Fig. 5a -2.9 (phase 2) +3.1 (phase 2)	no restrike +1.68 (phase 3); Fig. 5b -1.04 (phase 1)
B	+1.5 (phase 1) -2.5 (phase 2) +1.7 (phase 2)	+1.05 (phase 3) +1.18 (phase 1) +1.34 (phase 2)

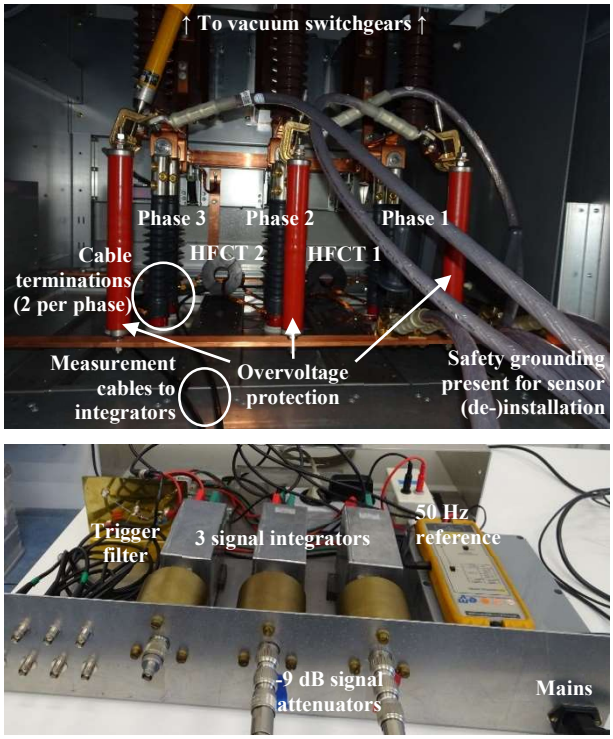

Fig. 6 – Compartment with the HFCT sensors (top) and the "EMC-shielding plate" with integrators (bottom)

4. Case II: inductive measurement

The cables that connect the vacuum switchgears with the compensation coil are accessible in the compartment shown in Fig. 6. For each phase, there are two parallel cables with their earth screens connected to ground. Two phases are monitored with two available HFCTs. Due to space restrictions, each HFCT could only be placed around the earth screen of one of the parallel cables.

The integrators, shown at the bottom of Fig. 6 are connected via 10 m long measurement cables. All connections, including the mains for powering the measurement equipment, are connected via the font of a shielding plate. This ensures that common mode currents find their way via this metal plate rather that via the measurement equipment. Besides the integrator signals, also the 50 Hz power frequency is recorded, which is extracted from the mains by means of a differential probe. This signal serves as reference to align the momentary phase angles of different measurements. A

trigger filter rejects the power frequency component and selects frequency components above 5 kHz. Triggering occurs on the fast transients from switching (on or off). The earth screen current represents the time derivative of the cable voltage. The cable capacitance C_{HV} (320 pF/m) acts as a voltage sensor, see Fig. 1d.

$$\left.\begin{aligned} i_{ch}(t) &= C_{HV}\frac{\mathrm{d}u_{HV}(t)}{\mathrm{d}t} \\ u'(t) &= i_{ch}(t)Z_{hfct} \\ u(t) &= \frac{A_{att}}{\tau_{int}}\int u'(t)\mathrm{d}t \end{aligned}\right\} \Rightarrow u(t) = A_{att}\frac{Z_{hfct}C_{HV}}{\tau_{int}}u_{HV}(t) \quad (2)$$

For estimating the measurement sensitivity with (2), it is assumed that the applied HFCT has a constant transfer Z_{hfct} (0.1 Ω, see Fig. 7). A -9 dB attenuator (A_{att}=0.355) in front of the integrator limits the signal amplitude such that 1 p.u. corresponds to about 0.5 V integrator output voltage. Signal clipping in the active part of the integrators only occurs above five times this value. The bandwidth is 20 MHz, but due to the cable length (30-40 m, making up C_{HV}) traveling waves may distort proper detection of frequencies above several megahertz.

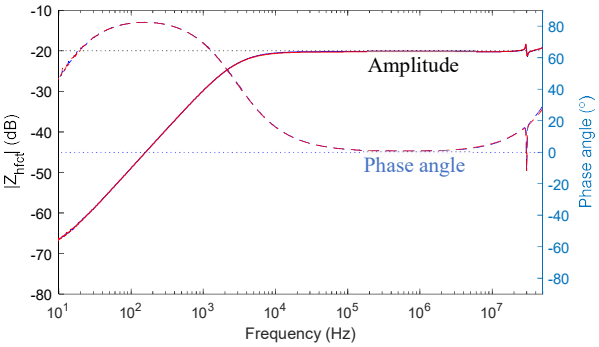

Fig. 7 – NA calibration of the HFCT responses

4.1. Signal manipulation

Although the HFCT response is rather constant as from about 5 kHz, the measured waveforms are corrected based on the measured transfer. Fig. 7 shows the calibration with a network analyser (NA).

Fig. 8a shows a de-energization event. There are a few problems in its recording, namely the power frequency components of the two phases are not equal in amplitude and, according to the low sensitivity of the HFCTs at 50 Hz (Fig. 7), these components should not be visible on this scale. As discussed in Section 2, most of the signal interference will arise at the measurement cable end with the highest impedance. As the HFCT represents a very low impedance (below 1 Ω), this is at the receiving end. This is different from the capacitive measurement in Section 3. The high 50 Hz component arises from the about 1 kA current to the compensation coil when it is energized. This current flows nearby the measurement cables and coupling occurs via the transfer impedances.

For higher frequencies, the problem vanishes because the HFCT becomes more sensitive and, due to the differentiating measurement, the earth screen current increases proportional to the frequency. Therefore, digital high-pass filtering is applied with a cut-off frequency of 500 Hz. The high frequency transients during one power cycle around the de-energization moment are shown in Fig. 8b. The power frequency component is eliminated from the signal. This means that normalizing the signal on the power frequency amplitude is not possible. It is now based on the initial amplitude of the decaying oscillation when a phase interrupts. This is about 1 p.u. as observed in Fig. 5b. The power frequency waveform, indicated as dashed sinewaves, is estimated on this normalization and with the assumption that an interruption occurs near current zero (i.e. maximum voltage for an inductive load). When evaluating (2), this sensitivity corresponds to C_{HV}=13 nF, which corresponds to about 40 m power cable length. This normalization is performed once and applied to all measurements.

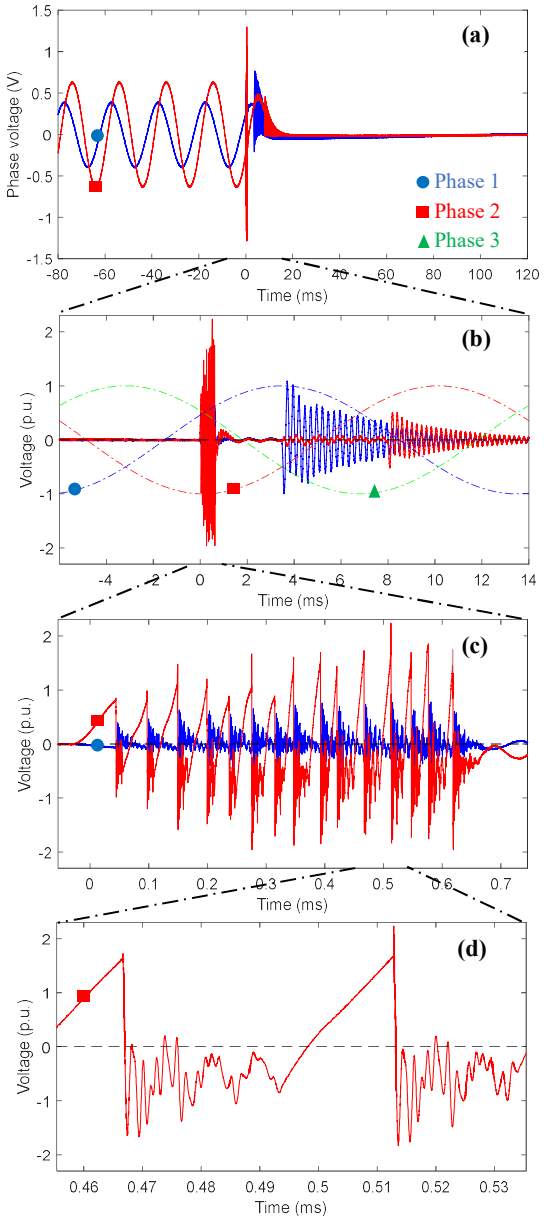

Fig. 8 – Waveforms from the HFCT sensors: (a) recorded signal, (b) filtered phase voltage during one 50 Hz cycle, (c) zoomed part around restrikes, (d) zoomed restrike event at phase 2; Note, no HFCT is installed at phase 3

Table 2 – Peak voltages registered during de-energization with involved phases and number of restrikes; 1 p.u. is added to the transient amplitudes (occurring near 50 Hz maxima)

Recording	Peak voltage de-energization (p.u.)	Number of restrikes
Tests after sensor installation	---	none
	+1.8 (phase 1)	21
	---	none
	+2.2 (phase 2)	13
	---	none
During three weeks of monitoring	+1.9 (phase 2)	21
	---	none
	-3.0 (phase 2)	15; Fig. 8
	---	none
	-?.? [1] (phase 3)	16

[1] Phase 3 is not monitored, but the restrikes are apparent from the responses observed in the two other phases

4.2. Switching overvoltages

The "L-C" oscillations involve the coil inductances and the cable capacitances and result in a 4.0 kHz component after interrupting the first phase and 4.8 kHz when the other phases interrupt. The waveform during the restrikes is shown in more detail in Fig. 8c. Each restrike can be recognized by an initial drop in the phase voltage when the contact is interrupted near current zero. A restrike causes an oscillation with typically a frequency of 500 kHz, see Fig. 8d. The restrikes repeat until interruption cannot take place anymore in the involved phase as the current has become too large meanwhile.

The peak voltages, summarized in Table 2, consider that the restrike occurs near a voltage extreme. So, 1 p.u. is added to the transient amplitude. In 50% of the de-energization events, restrikes were recorded prior to the interruption and these events are responsible for the highest values. In addition, they have steep fronts, e.g. a variation up to 4 p.u. within 1 µs as shown in Fig 8d.

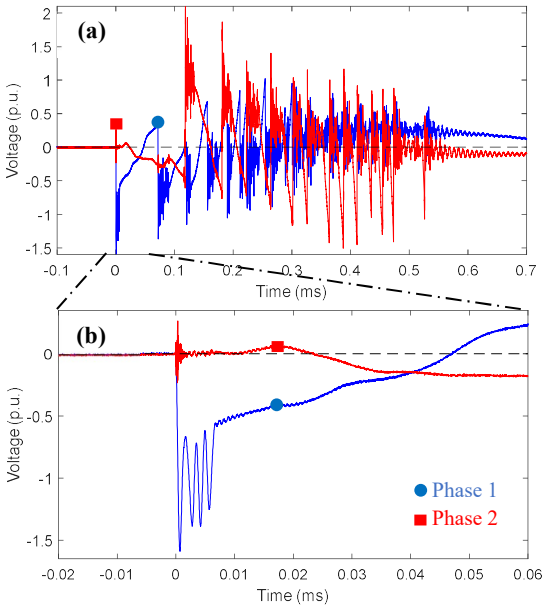

Fig. 9 – Waveforms at two phases (a) during energization and (b) zoomed signal around the first prestrike

Closing of the switchgear contacts is accompanied by prestrikes. The highest recorded overvoltage is shown in Fig. 9a. At $t = 0$, phase 1 exhibits prestrikes until full contact is established after about 0.5 ms. Prestrikes in phase 2 starts a $t = 0.12$ ms. The oscillation frequency after a prestrike is about 500 kHz, Fig. 9b.

5. Conclusion

Switching an inductive load can cause high overvoltage levels. These overvoltages are usually expected from the potentially high dI/dt during de-energization. However, the highest value (exceeding 3 p.u.) was observed during the energization in case of the SF_6 switchgear.

The highest overvoltages during the de-energization occur upon the restrikes. In most cases for the SF_6 switch, a single restrike occurred close to a zero current moment in one phase, and final interruption took place after the successive zero crossing in one of the other phases. With the vacuum switch, in half of the recorded events multiple restrikes occurred.

In particular, the de-energization transients from vacuum switchgears can severely stress dielectric materials in network components. The restrikes during switching can cause transients with rise times below 1 µs, i.e. faster than waveforms applied in component testing with lighting surges. The restrikes can repeat several tens of times, meaning that they extend for a duration typically for front times in waveforms used for testing upon switching surges. In addition, these restrikes occur when the power frequency amplitude has reached its maximum. It may therefore be questioned, whether testing the voltage withstand capability of a grid component with separate power, switching and lightning voltages is sufficiently representative for the waveforms occurring during actual switching of an inductive load.

6. References

[1] A.P.J. van Deursen, H.W.M. Smulders, R.A.A. de Graaff, "Differentiating/integrating measurement setup applied to railway Environment", *IEEE Transactions on Instrumentation and Measurement*, Vol. 55, No. 1, 2006, pp. 316-326.

[2] E. Kuffel, W.S. Zaengl, J. Kuffel, "*High Voltage Engineering: Fundamentals*", 2nd ed Newnes, 2000.

[3] P.C.T. van der Laan, A.P.J. van Deursen, "Reliable protection of electronics against lightning: some practical applications", *IEEE Transactions on Electromagnetic Compatibility*, Vol. 40, No. 4, 1998, pp. 513-520.

[4] P. Wouters, A. van Deursen, M. Vermeer, "Methodology and accuracy for non-invasive detection of switching transient overvoltages from compensation coils connected to power transformers", *IET Science, Measurement & Technology*, Vol. 14, No. 2, 2020, pp. 173-181.

[5] FCC, https://www.fischercc.com/products/f-40-5/, last accessed 17-02-2022.